Deep-Sea Research I 58 (2011) 745–756

Contents lists available at ScienceDirect

Deep-Sea Research I

journal homepage: www.elsevier.com/locate/dsri

The Arctic Ocean halocline and its interannual variability from 1997 to 2008

P. Bourgain *, J.C. Gascard

LOCEAN/IPSL, Université Pierre et Marie Curie, Paris, 75005, France

A R T I C L E I N F O

Article history:
Received 16 December 2010
Received in revised form
20 April 2011
Accepted 5 May 2011
Available online 19 May 2011

Keywords:
Arctic Ocean
Halocline
Water masses
Physical oceanography

A B S T R A C T

As a key structure to understand the role of the ocean on the sea ice mass balance, the Arctic Ocean halocline and its spatiotemporal variability require serious attention. In this paper, we are proposing a new definition of the halocline, which is based on the salinity gradient structure, taking into account both the salinity amplitude and the thickness of the halocline. The Brunt Vaisala frequency is used as the halocline stratification index. CTD data collected from 1997 to 2008 and coming from various sources (icebreaker cruises, drifting buoys, etc.) are used to determine the halocline, and its time and space variability during three time periods, with a special focus on three main regions of the Arctic Ocean: the Canada basin, the Makarov basin and the Amundsen basin. Observations reveal that the halocline in the Amundsen basin was always present and rather stable over the three time periods. In contrast, the Canada and Makarov basins' halocline became more stratified during the IPY than before, mainly because of surface water freshening. In addition, observations also confirmed the importance of the halocline thickness for controlling the stratification variability. Observations suggest that both large scale and small scale processes affect the halocline. Changes in surface salinity observed in the Makarov basin are more likely due to atmospheric variability (AO, Dipole Anomaly), as previously observed. More locally, some observations point out that salt/heat diffusion from the Atlantic water underneath and brine rejection during sea ice formation from above could be responsible for salt content variability within the halocline and, as a consequence, being influential for the variability of the halocline. In spite of the existence of interannual variability, the Arctic Ocean main stratification, characterized by a stable and robust halocline until now, suggested that the deep ocean had a limited impact on the mixed layer and on sea ice in actual conditions. The drastic changes observed in Arctic sea ice during this period (1997–2008) cannot be attributed to a weakening of the halocline that could trigger an enhanced vertical heat flux from the deep ocean.

1. Introduction

Arctic sea ice underwent some dramatic extent and thickness reduction in recent decades: 30% of the summer sea ice extent was lost in 30 years (the September sea ice decline rate is 10% per decade since 1979, according to NSIDC) and its thickness in winter diminished by 1.75 m over 25 years (Kwok and Rothrock, 2009). Even if the atmospheric forcing is clearly involved in this drastic reduction, it would explain only 40% of the observed sea ice extent reduction (Francis et al., 2005), leaving a substantial role to the oceanic forcing. The halocline, a thick layer (100–200 m) characterized (by definition) by a strong salinity gradient structure that lies between the surface convective mixed layer above and the warm underlying Atlantic water layer underneath, is considered to be an insulating "density barrier" between this major heat reservoir at depth and the mixed layer and sea ice above. As such, the halocline is a key feature regulating the impact of the ocean on the sea ice mass balance.

Two main mechanisms were proposed to explain the formation of this layer. Aagard et al. (1981) proposed an advective origin: ice growth on the shelves produces brine that sinks to the base of the shelves before being advected toward the deep basins. This process generates a cold and salty water mass, the "Cold Halocline Layer", at intermediate depths, between the mixed layer and the Atlantic water. Rudels et al. (1996) proposed that winter convection homogenizes the upper part of the Atlantic water from the surface down to the thermocline up to the Laptev Sea where Siberian river run-off provides a freshwater cap at the top of the water column. As a result, the surface stratification increases and limits the winter convection to a thin layer at the surface which becomes the mixed layer; and the salty and cold water below becomes isolated from the surface.

Once formed, the halocline water is advected by the main oceanic circulation and is subjected to different influences (Fig. 1—left panel). At surface, the mixed layer salinity is impacted by the river run-off,

* Corresponding author. Tel.: +33 144278452.
E-mail addresses: Pascaline.Bourgain@locean-ipsl.upmc.fr (P. Bourgain), Jean-Claude.Gascard@locean-ipsl.upmc.fr (J.C. Gascard).

0967-0637/$ - see front matter © 2011 Elsevier Ltd. All rights reserved.
doi:10.1016/j.dsr.2011.05.001

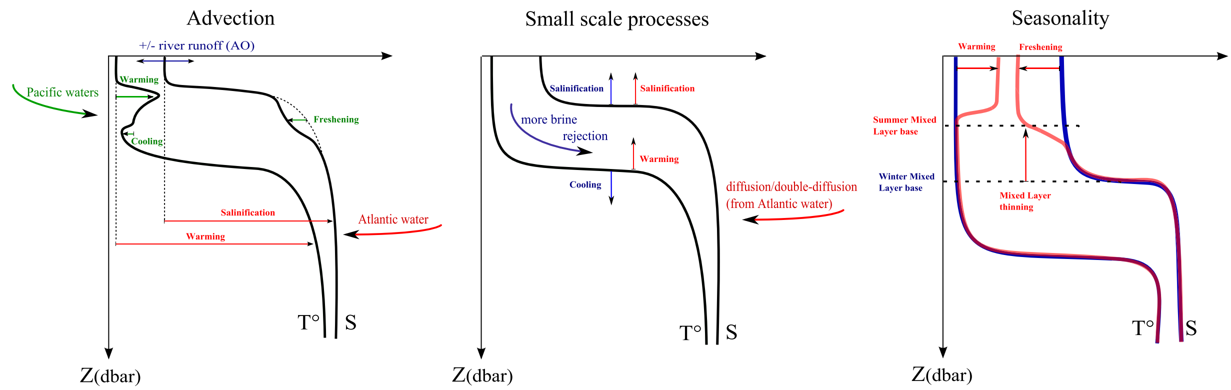

Fig. 1. Schematic views of the different processes influencing the Arctic Ocean halocline: advection (left panel), small scale processes (mid panel), seasonality (right panel). On the advection scheme, the effects of the river runoff, the advection of Pacific waters and Atlantic waters are represented in blue, green and red, respectively. On the small scale processes scheme, the effects of the brine rejection and diffusion/double diffusion are represented in blue and red, respectively. The seasonality scheme focuses on the upper layers of the water column. The blue and red profiles correspond to winter and summer type profiles, respectively. Only the effects of the summer are represented in red (as the winter effects are in direct opposition to the summer effects). (For interpretation of the references to color in this figure legend, the reader is referred to the web version of this article.)

which is directly affected by surface winds (Arctic Oscillation, AO). For instance, a high AO index results in an eastward component of the winds over the Laptev Sea driving the fresh Siberian shelf waters from the Eurasian basin to the Makarov basin (Steele and Boyd, 1998). The relatively fresh waters originating from the Pacific and entering the Arctic Ocean through Bering Strait, influence the salinity gradient profile of the Canadian basin halocline (Shimada et al., 2005; Steele et al., 2004) explaining why typical Eurasian basin and Canadian basin haloclines have a different shape (see Fig. 6—left panel). Moreover, depending on the season, Pacific waters influence the halocline by introducing either a shallow temperature maximum near 50 m depth (the Summer Pacific waters) or a deeper minimum temperature around 100 m depth (the Winter Pacific waters). These Pacific waters are not present in the Eurasian basin. The warm and salty Atlantic waters entering through Fram Strait or crossing the Barents Sea, influence the Arctic water column stratification at greater depths (300–800 m) (Rudels et al., 1996) and constitute the main reservoir of heat for the whole deep Arctic basin. They are an important source of heat and salt for the Lower Halocline waters.

In addition, the halocline can also be affected by local processes such as diffusion or double diffusion, triggered by the presence of strong temperature and salinity gradients due to warm and salty waters underlying fresher and colder waters above (Fig. 1—middle panel). Actually, a stronger Atlantic water mass can lead to a warming and a salinification of the interface between the Atlantic layer and the halocline (Polyakov et al., 2010) and decrease the temperature gradient in the upper part of the thermocline.

Finally, the top of the halocline (underneath the mixed layer base) is strongly affected by seasonal processes (Morison and Dungan Smith, 1981). During the winter, brine rejection (Fig. 1—middle panel) resulting from sea ice formation, implies a cooling and a salinification of the upper layers of the water column. Convection (Fig. 1—right panel) deepens the mixed layer and could, in absence of the halocline, reach the thermocline and increase the temperature gradient in the upper part of the thermocline (Rudels et al., 1996, 2004; Kikuchi et al., 2004). When the melting season begins, the fresh water due to sea ice melting covers the surface layer and, as a result, the mixed layer is much thinner than during the winter. Consequently, the upper ocean stratification increases significantly during the summer. Moreover, incoming solar radiation trapped by the ocean surface layer increases the sea surface temperature and the upper ocean heat content. There appears a temperature maximum very near the surface (Toole et al., 2010) but well above the first temperature maximum at about 50 m depth related to Summer Pacific water.

According to Steele and Boyd (1998), the halocline underwent some drastic changes in the early 1990s and even disappeared from time to time. They based their analysis on a "salinity tracer for the presence or absence of the cold halocline layer" (CHL). According to them and based on this tracer definition, the CHL "disappeared" from the Eurasian basin during the early 1990s due to a shift in the atmospheric wind forcing that would have changed the destination of the fresh Siberian shelf waters flowing into the deep Arctic Ocean. Boyd et al. (2002) and Bjork et al. (2002) evidenced a "partial recovery" of the Arctic cold halocline in the late 1990s.

As a key feature to understand the role of the ocean on the sea ice mass balance, the Arctic Ocean halocline and its spatiotemporal variability requires serious attention. This paper addresses two important questions: (1) Do we have a reliable definition of the Arctic Ocean halocline and if not, how can we best define it? (2) Is the Arctic Ocean halocline highly variable in the context of a highly variable Arctic sea-ice cover as observed during recent years? If that was the case, one might suspect the warm water masses circulating within the upper part of the halocline (the Summer Pacific water) and deeper underneath the halocline (the Atlantic Water) to contribute significantly to the drastic sea-ice melting observed during recent years.

In the following, based on a large data set collected in the central Arctic basin from 1997 to 2008 during several field campaigns, the definition of the halocline and the choice for an appropriate halocline tracer and index will be discussed. Then, the paper will focus on the halocline spatiotemporal variability observed during the past 11 years as a prerequisite for estimating the potential contribution of the oceanic heat flux to sea-ice melting (not part of this paper).

2. Data and method

2.1. Data collection

Thanks to a remarkable cooperation among Arctic scientists from many countries, more than 18,000 CTD vertical profiles were collected from 1997 to 2008 in the deep Arctic Ocean (Table 1). It includes data from icebreaker campaigns, from drifting platforms and even from aerial survey and submarine cruises. Note that observations collected in shallow waters (Arctic shelves) are not included in this study. Noticeably, about two thirds of the data set were collected during the fourth International Polar Year, in 2007–2008 (Fig. 2).

2.2. Data processing

2.2.1. Standard processing

After removing outliers, the data set, extending from near surface down to 1000 decibar (dbar) level, was interpolated each 1 dbar. The density and the potential temperature were calculated using UNESCO 1983 tables. Raw gradients were obtained from the differences between two successive values sampled 1 dbar apart. Moreover, smoothed variables and gradients are required for detecting the halocline upper and lower parts as described in Section 3.2. We applied a moving average filter. For instance, in case of the halocline base detection, both the potential temperature (salinity) and temperature (salinity) gradient were smoothed through a moving average over the 10 surrounding data points. For the detection of the mixed layer base, a moving average over 6 surrounding data points rather than 10 was applied to the variables because a better precision was required.

Table 1
Data set by cruises, time and location.

Data set	Time	Location
SHEBA (1 profile per day)	Autumn 1997–Autumn 1998	Canada basin
SCICEX	Autumns 1997–1998–2000	Central basin
AMORE	Summer 2001	Gakkel Ridge
ODEN	Summer 2001	Eurasian basin
Polar Observer	Spring 2002	Amundsen basin
JWACS	Autumn 2002	Beaufort Sea
ARK XX2	Summer 2004	Fram Strait
BERINGIA	Summer 2005	Central basin
POPS IPEV	2006–2007	Central basin
LOMROG	Summer 2007	Fram Strait
ARK XXII2	Summer 2007	Eurasian and Makarov basins
NABOS	Summers 2002 to 2007	Laptev Sea
Akademik Fedorov	Summer 2007	Laptev Sea and Canadian basin
Akademik Fedorov	Summer 2008	Laptev Sea
NP 35	Autumn 2007–Spring 2008	Nansen basin
CHINARE	Summer 2008	Beaufort Sea
ARK XXIII3	Summer–Autumn 2008	Mendeleyev Ridge
NPEO Aerial Survey	Springs 2000–2008	Central basin
TARA	Autumn 2006–Winter 2008	Central basin
POPS JAMSTEC 9, 11	Autumn 2008	Makarov basin
ITP 1–30	Summer 2004–Winter 2008	Central basin

2.2.2. Interpolation via Kriging

Some of the following maps were obtained using the Kriging method. It is a geostatistical technique to interpolate the value of a random field from observations at nearby locations. It is an improvement over all other interpolation methods because it minimizes error covariance. This method was used to construct spatial maps on a 1°longitude × 0.5°latitude grid of several parameters first estimated from original T and S profiles. We chose the ten closest points within a certain radius to be the Kriging interpolation neighborhood. The minimum radius was determined by the range of the variogram (Krige, 1951; Matheron, 1963); depending on the variable interpolated, it was running from 300 to 500 km. Note that the variance of the sum of two variables being not equal to the sum of the variance of each variable, we obtain for the Kriging interpolation: $K(a+b) \neq K(a)+K(b)$, with a and b two variables and K the Kriging operator.

This method was applied to summer data only (early July to late September) in order to avoid seasonal bias that could have strongly affected the results about interannual variability. This data set was split into three time periods determined after several tests: the first period runs from 1997 to 2002 (referred as period 1), the second period, from 2003 to 2006 (referred as period 2) and the third period, from 2007 to 2008 (IPY, referred as period 3). Although a discrepancy of the data still remains, this combination appeared to be the best compromise to get both a sufficient number of data with the best spatial distribution, i.e. a higher spatial interpolation pattern and a short time period to obtain the best time resolution. In point of fact, before IPY, most of the data were only collected during the summer because of harsh winter conditions. It was only with the recent deployment of drifting buoys (ITPs, POPS, etc.) that a large collection of winter data was made possible. The interannual variability inside these time periods is ignored so all available data over the whole time period for the summer months is used.

For period 1 and period 3, the data are well distributed over the years (Fig. 3). Note that there is no summer data during years 1999 and 2000. On the contrary, during period 2, the data were mostly collected in 2006. Hence, there is a bias in time for that period. The IPY map is the one with the highest confidence level

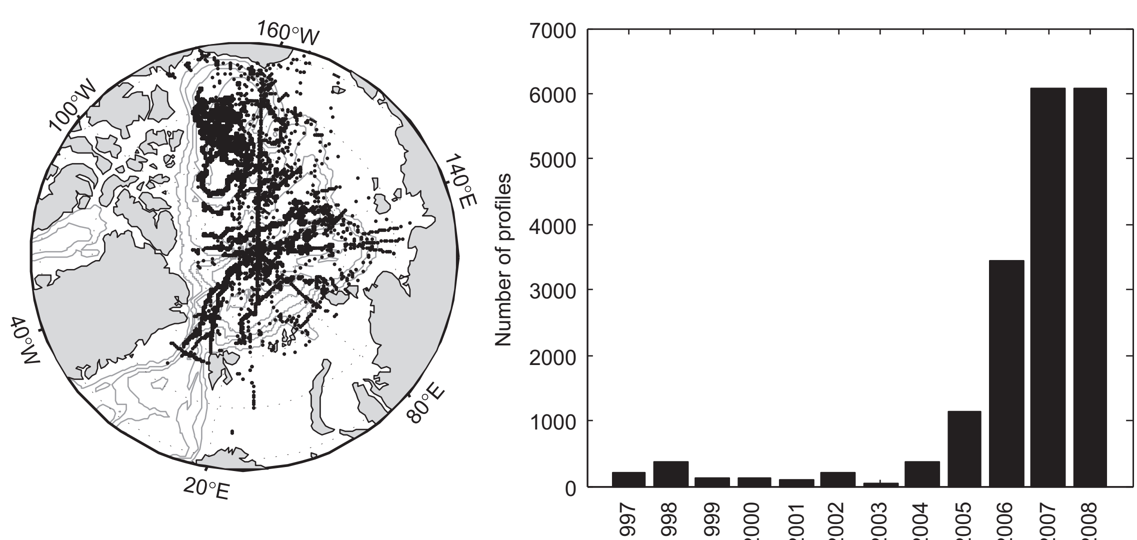

Fig. 2. Spatial distribution of the data set (left) and histogram of the annual number of data (right).

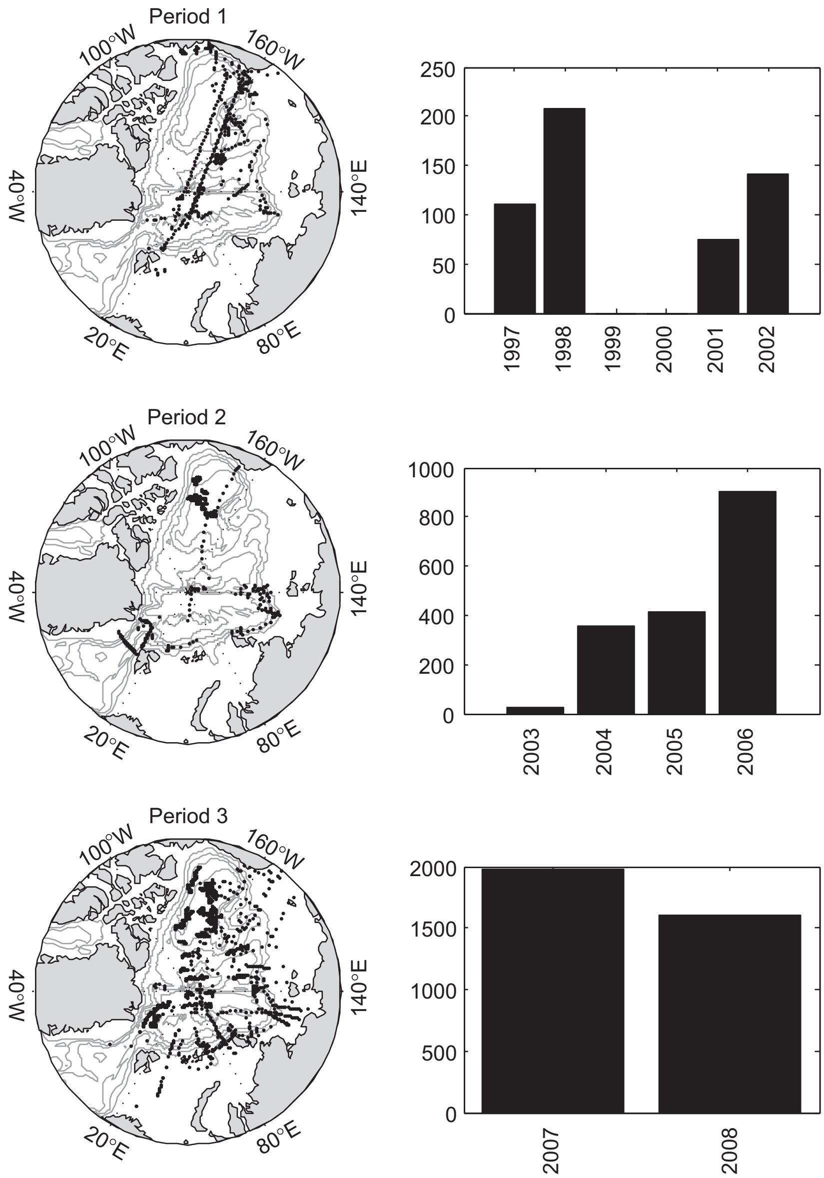

Fig. 3. Spatial distribution of summer data and the corresponding histogram for the three time periods.

because of the highest density of data. Moreover, for the three time periods, the less documented geographical zone is the region close to the Canadian archipelago, which is less accessible due to thicker ice all year around.

3. Algorithm for halocline characterization

3.1. Steele and Boyd's halocline "tracer" (S_{SB})

Steele and Boyd (1998) proposed the mean salinity of the 40–60 m layer depth (referred as S_{SB}) to be "a tracer for the presence or absence of a CHL (Cold Halocline Layer)". In case $S_{SB} \geq 34$ psu, the CHL is absent whereas for $S_{SB} < 34$ psu, the CHL is present. Based on this tracer, the halocline "retreat" from the Amundsen basin was observed in the early 1990s and its "partial recovery" (because the isohaline 34 psu did not come back to its pre-1990s location into the Amundsen basin) was observed in the late 1990s (Boyd et al., 2002; Bjork et al., 2002). Is S_{SB} a relevant tracer for the halocline?

Steele and Boyd chose S_{SB} as the CHL's tracer because according to them, this corresponded to the deepest winter mixed layer salinity in the Eurasian basin. However, they based this information on a small data set that might not be a good representative of the Eurasian basin. In point of fact, the larger data set collected during IPY reveals the existence of a very thick mixed layer (Fig. 4) in the Amundsen and Nansen basins (> 70 dbar). As a consequence, the same salinity at 40–60 m depth can be recorded in water columns with different stratification. Moreover, the halocline thickness is not taken into account with Steele and Boyd halocline's tracer definition. Consequently, S_{SB} is not well adapted to represent the halocline.

3.2. The Brunt Vaïsala frequency: an index for the Arctic halocline

Until now, the halocline had been detected most of the time either by a salinity constant or salinity range (Steele et al., 1995) either by a depth range (Boyd et al., 2002; Steele and Boyd, 1998). Rudels et al. (1996) was among the few who defined the halocline as a layer, using a minimum temperature due to winter convection to detect the top of the halocline and a salinity constant to

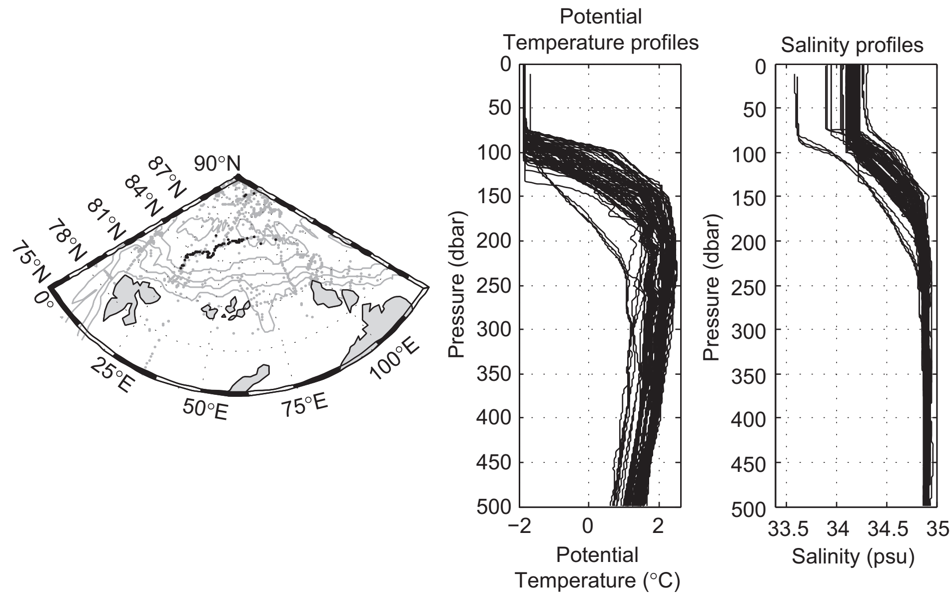

Fig. 4. Location of the very deep mixed layers (left) and their corresponding temperature and salinity profiles (right).

detect the base of CHL in the Eurasian basin. It was later elaborated by Rudels et al. (2004) and Rudels (2010) that the choice of the salinity constant depends upon the temperature and salinity of the underlying Atlantic water. In the following, we will consider the halocline as a thick layer constrained by its upper and lower bounds, referred as its top and base. Moreover, we are looking for a Pan Arctic general definition of the halocline not restricted to the Eurasian and/or the Canadian basin only.

We propose a new definition of the halocline based on the fact that it is (by definition) mainly characterized by a salinity gradient structure. The top of the halocline is chosen just below the base of the mixed layer. This depth is detected by the "gradient method", when both the smoothed temperature vertical gradient and salinity vertical gradient jump from zero to a significant value.

In addition, we propose to define the base of the halocline as a maximum ratio of density gradient due to temperature to the density gradient due to salinity (rather than a salinity constant), in order to capture the transition from a halocline to a thermocline. This ratio R is defined as follows:

$$R=\alpha\Delta T/\beta\Delta S,$$

with α, the thermal expansion coefficient and β, the haline contraction coefficient. ΔT and ΔS are the smoothed temperature and salinity variations over one decibar. A low value of R corresponds to a weak vertical temperature gradient and a large vertical salinity gradient, which is characteristic of the halocline structure. Inversely, a larger value of R, with a larger vertical temperature gradient and a weaker vertical salinity gradient, is characteristic of the thermocline structure. It is critical to find a ratio that is pertinent and that sets up the halocline base close to the "elbow" of the TS diagram, well-known in the literature as being the Lower Halocline waters (Jones and Anderson, 1986; Kikuchi et al., 2004; etc.). The distribution of all the profiles in the Temperature–Salinity (TS) space indicates that the "elbow" is well represented through a ratio ranging from 0.03 to 0.07. $R=0.05$ corresponds to the best fit for the halocline base because, compared to other values, it is the ratio that gives the smallest standard deviation for pressure, temperature and salinity (Fig. 5).

Once the halocline top and base boundaries are established, the square of the Brunt Vaïsala frequency (referred as N^2) averaged over the whole halocline layer is used to determine the halocline stratification index. This index takes into account both the halocline salinity amplitude and the halocline thickness as well. Moreover, N^2 is quite convenient as it permits to characterize all types of haloclines, not only the Eurasian Cold Halocline but also the Canadian haloclines.

In summary, three elements characterize the Arctic halocline:

1. The depth $H1$ at the base of the surface mixed layer, i.e. at the top of the halocline, for a given salinity $S1$ and potential density $\rho 1$.
2. The depth $H2$ at the base of the halocline characterized by a density ratio of 0.05 and corresponding to a salinity $S2$ and a potential density $\rho 2$.
3. The halocline stratification index (N^2, in s^{-2}) is proportional to the difference in potential density between the end points of the interval divided by the depth span

   $$N^2=(g/\rho)((\rho 2-\rho 1)/(H2-H1))$$

   with g, the local acceleration of gravity and ρ, the potential density.

Moreover, at cold temperatures, the density is mainly controlled by the salinity. Therefore, in first approximation, the halocline stratification N^2 is mainly proportional to the salinity gradient, which is proportional to the salinity amplitude ($S2-S1$) and inversely proportional to the halocline thickness ($H2-H1$).

Fig. 6 gives a representation of one typical salinity profile for both the Eurasian and Canadian basin (left panel). One can see that the Canadian halocline is much thicker than the Eurasian one. While the Eurasian basin halocline only shows a single peak of stratification just below the mixed layer, the Canadian basin halocline exhibits a double peak, the second being deeper and weaker and resulting from the junction with the Atlantic waters below (right panel). The minimum stratification between the two peaks is due to the influence of the relatively fresh winter Pacific waters that enters the Canadian basin halocline at mid-depth.

In the following section, we will investigate the evolution of the halocline parameters ($H1$, $H2$, $S1$ and $S2$) during the past 11 years.

4. Arctic halocline variability over the past 11 years

The evolution of the halocline stratification during the three selected periods is represented in Fig. 7. The most stratified Arctic

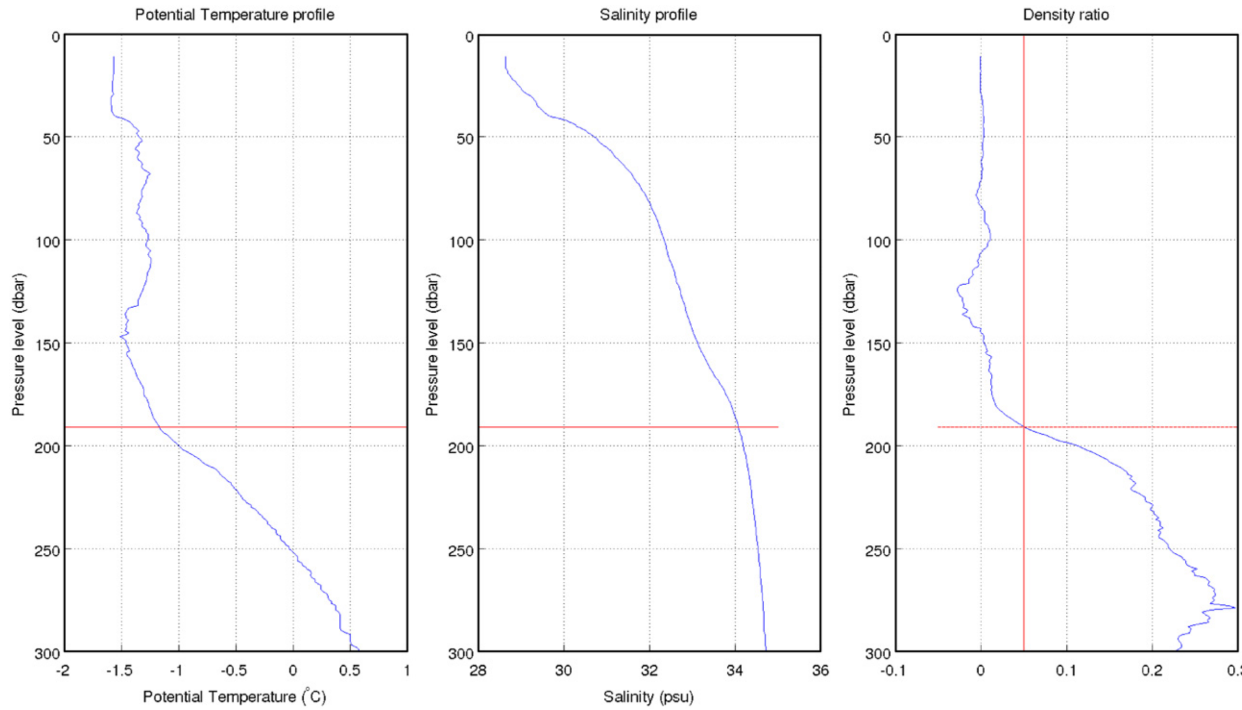

Fig. 5. Example of the detection of the halocline base with the density ratio method. The base immersion is indicated on the three profiles by horizontal lines.

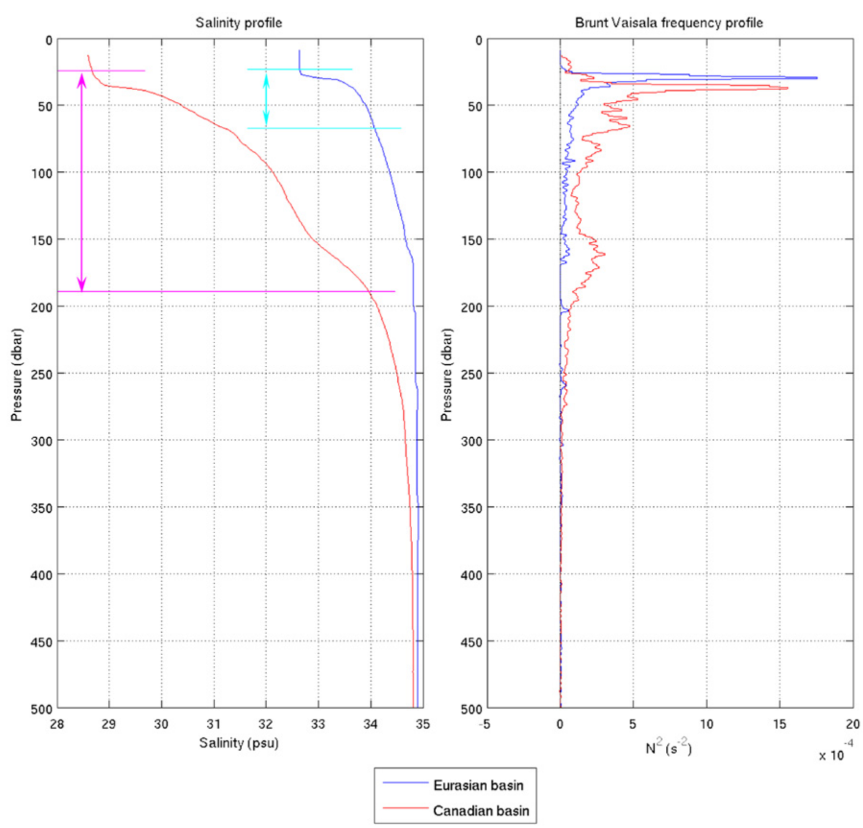

Fig. 6. Example of a salinity vertical profile (left panel) taken in the Canadian basin (red) and in the Eurasian basin (blue) and their corresponding N^2 vertical profile (right panel). The top and base immersions are indicated on the salinity profile by horizontal lines. (For interpretation of the references to color in this figure legend, the reader is referred to the web version of this article.)

haloclines are located close to the Siberian shelves due to the large freshwater input from Siberian river run-off at surface and the least stratified haloclines are located on the Western side of the Nansen basin. The latter also correspond to the location where very deep mixed layers were encountered (> 70 dbar, see Section 3.1).

The corresponding standard deviation is plotted in Fig. 8 in order to focus on the geographical areas with the highest

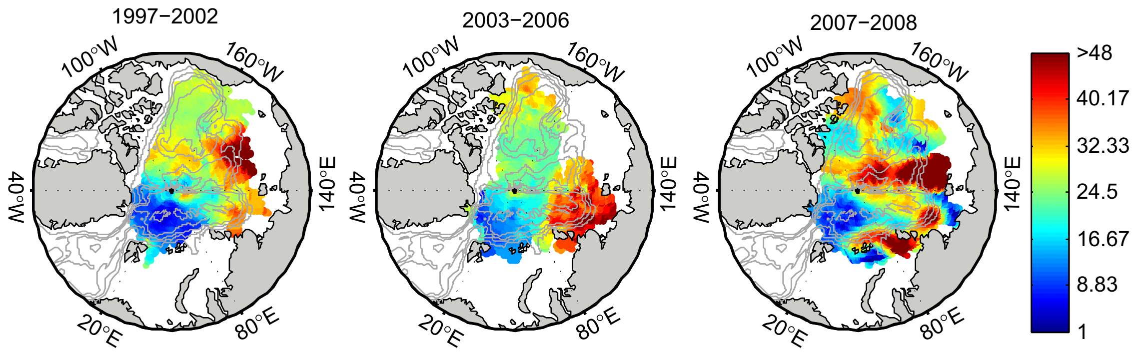

Fig. 7. The halocline stratification ($\times 10^{-5}\,s^{-2}$) evolution from period 1 to period 3. The black dot marks the location of the North Pole.

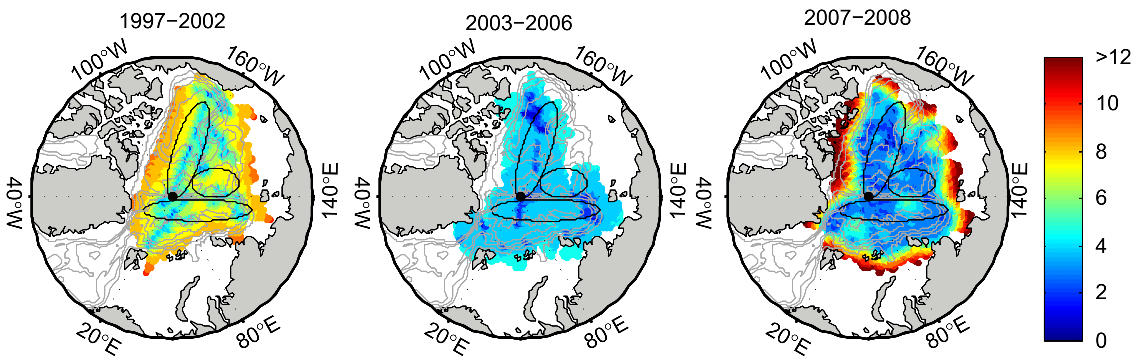

Fig. 8. Standard deviation of the halocline stratification ($\times 10^{-5}\,s^{-2}$) evolution from period 1 to period 3. The black dot marks the location of the North Pole. The ellipses locate the three regions selected for a detailed analysis.

confidence level. Three main areas were selected – located by ellipses on the maps – corresponding to a reasonable standard deviation of the three time periods: the Canada basin, the Makarov basin and the Amundsen basin. These three areas cover the main regions of the Arctic Ocean, providing some representation of the overall situation in the Arctic Ocean.

In the following, we will investigate the respective contributions of the different halocline parameters to the halocline stratification variability during the past 11 years in the three selected regions: the Canada basin, the Makarov basin and the Amundsen basin (see Figs. 9 and 10, and Table 2).

4.1. Halocline variability in the Canada basin

The stratification of the Canada basin halocline was rather stable during P1 and P2 but increased strongly during the IPY. N^2 remained close to $25\times10^{-5}\,s^{-2}$ during P1 and P2 in spite of a small increase of the salinity amplitude with time due to a slight freshening at the surface (the halocline salinity at the base was rather stable and close to 34.1 psu). The thickening of the halocline, from 73 to 91 dbar, due to the uplift of the top of the halocline, balanced the salinity change. During the IPY, the halocline thickness did not change significantly compared to P2 because both the halocline top and base got deeper. The salinity amplitude contributed to an increase of stratification (up to $N^2=35\times10^{-5}\,s^{-2}$) with a drop of the surface salinity by almost 1.6 psu (from 30.3 to 28.7 psu).

4.2. Halocline variability in the Makarov basin

In the Makarov basin, the situation was quite similar to the situation in the Canada basin. The halocline stratification was quite stable in the first two time periods ($N^2=29\times10^{-5}\,s^{-2}$ and $N^2=28\times10^{-5}\,s^{-2}$, respectively), but during IPY, the increase of the stratification was particularly important, reaching $N^2=45\times10^{-5}\,s^{-2}$. Even with some changes in the halocline thickness ranging from 73 dbar during P1 to 88 dbar during P3, the salinity amplitude was definitely responsible for the halocline stratification variability. The Makarov basin encountered a strong freshening of its surface layers during recent years compared to the previous years: the surface salinity decreased from 31.4 psu during P1 to 31.2 psu during P2 and 29.1 psu during P3.

4.3. Halocline variability in the Amundsen basin

In the Amundsen basin, the halocline was quite steady over the three time periods compared to the situation in the Canada and Makarov basins. The strongest stratification of the halocline was met during P2 with $N^2=23\times10^{-5}\,s^{-2}$ while the smallest value was met during P1 with $N^2=17\times10^{-5}\,s^{-2}$. The halocline top and base almost remained unchanged from P1 to P2 and therefore had no consequences on the halocline thickness. The increase in stratification from P1 to P2 was only due to a drop in the surface salinity from 32.7 to 32.1 psu. During the IPY, there was a continuous decrease in surface salinity, the stratification decreased slightly because the layer became thicker, from 68 to 77 dbar during P2 and P3, respectively.

5. Discussion

5.1. The atmospheric forcing and the surface salinity variability

The changes in the last decade in the Arctic Ocean have been partly attributed to the atmospheric forcing. For instance, as already mentioned in the introduction, anomalous wind forcing correlated with the Arctic Oscillation (AO) index influenced the region where

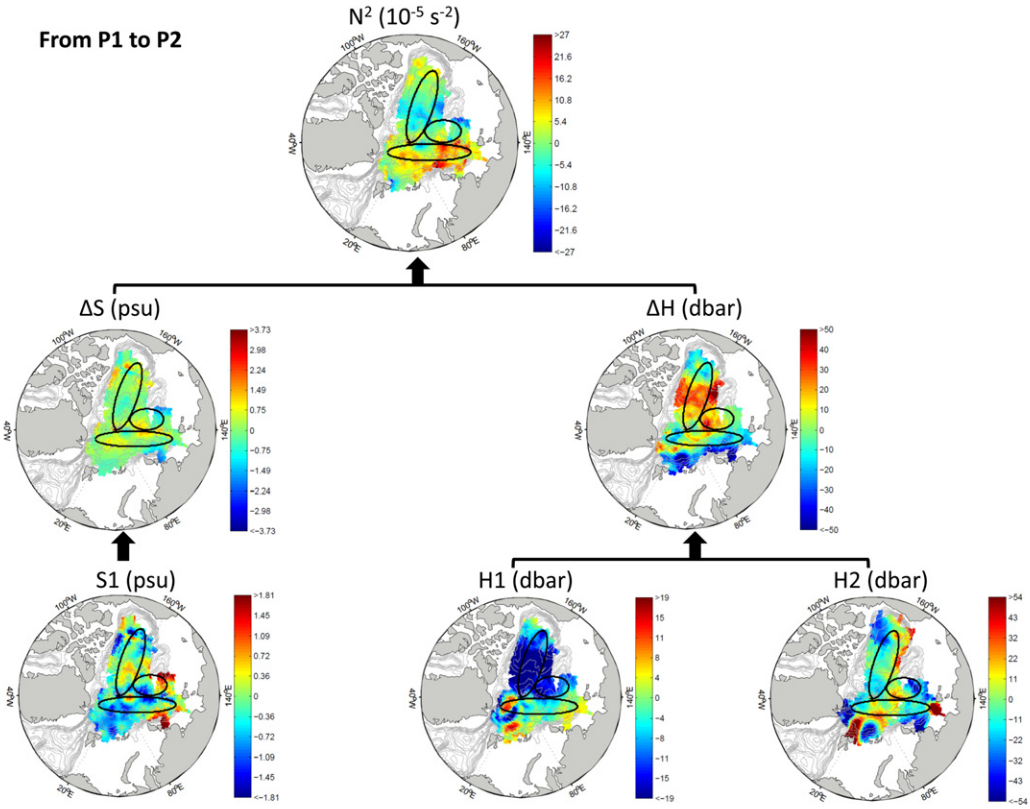

Fig. 9. Halocline features evolution from 1997–2002 (period 1) to 2003–2006 (period 2). These figures were obtained by subtracting the time periods between them. Blue colors correspond to a decrease in time of the concerned parameter while red colors correspond to an increase in time of the concerned parameter. (For interpretation of the references to color in this figure legend, the reader is referred to the web version of this article.)

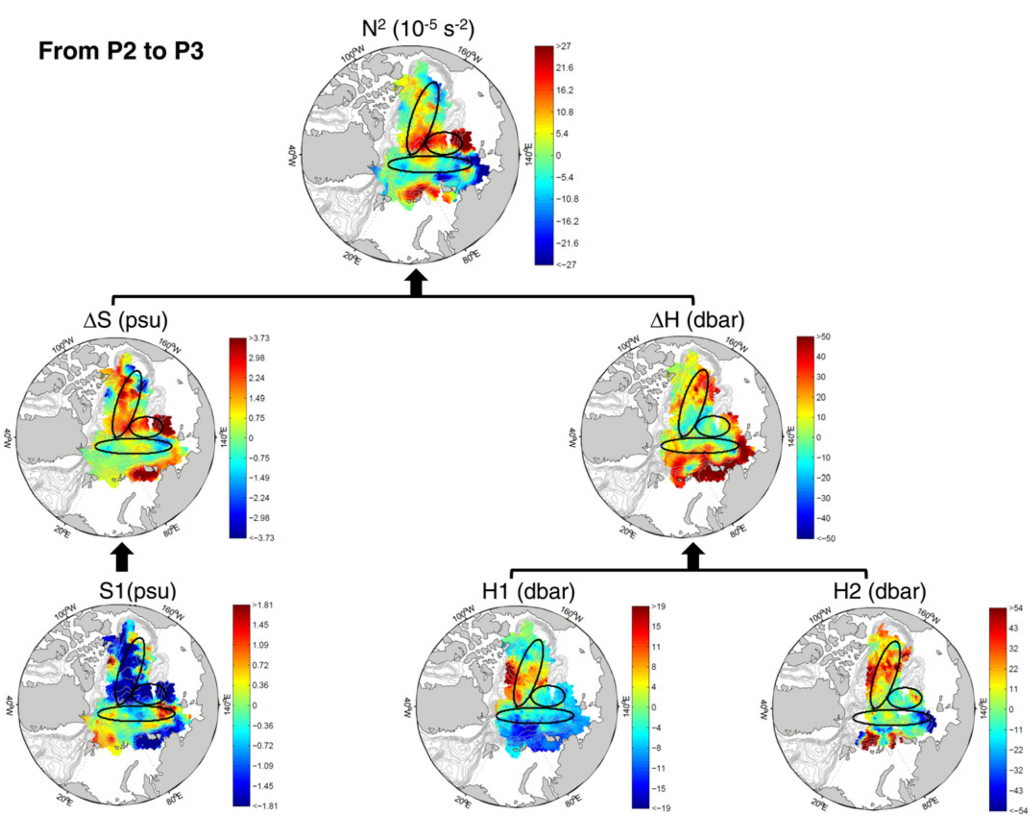

Fig. 10. Halocline features evolution from 2003–2006 (period 2) to 2007–2008 (IPY, period 3). These figures were obtained by subtracting the time periods between them. Blue colors correspond to a decrease in time of the concerned parameter while red colors correspond to an increase in time of the concerned parameter. (For interpretation of the references to color in this figure legend, the reader is referred to the web version of this article.)

Table 2
Spatiotemporal variability of the parameters affecting the halocline stratification averaged inside the selected regions. Corresponding standard deviations are indicated in brackets. $H1$, $H2$ and ΔH (dbar) correspond to the immersion of the halocline top and base and to the halocline thickness, respectively. $S1$, $S2$ and ΔS (psu) correspond to the salinity at the halocline top and base and to the salinity amplitude, respectively. $N^2(\times 10^{-5}\,s^{-2})$ corresponds to the measure of the halocline stratification as defined in Section 3.2. These calculations were made with data issued from the Kriging interpolation in order to avoid spatial and/or temporal bias. This is why the values of ΔH (or ΔS) are not equal to the difference between the values of $H2$ (or $S2$) and $H1$ (or $S1$), as previously explained in Section 2.2.2. However, this does not affect at all the analysis about the variability of the halocline. Note also that the standard deviations inside the three areas are elevated. This is because the areas investigated were deliberately chosen quite large in order to have a global approach of the situation in the Arctic Ocean. If reducing the size of each area investigated, the standard deviations would be reduced but as the conclusions would stay unchanged, we keep this regionalization of the Arctic Ocean.

Location	**Parameters**						
	$H1$ (dbar)	**$H2$ (dbar)**	**ΔH (dbar)**	**$S1$ (psu)**	**$S2$ (psu)**	**ΔS (psu)**	**N^2 ($\times 10^{-5}\,s^{-2}$)**
Canada basin							
P1	32 [7.1]	140 [10.3]	73 [14.2]	30.577 [0.624]	34.103 [0.065]	3.578 [0.652]	26 [5.9]
P2	12 [3.9]	131 [7.3]	91 [11.5]	30.323 [1.001]	34.083 [0.039]	3.769 [0.888]	25 [3.5]
P3	17 [4.4]	144 [12.2]	88 [8.6]	28.728 [0.447]	34.054 [0.111]	5.250 [0.345]	35 [3.0]
Makarov basin							
P1	29 [8.7]	103 [10.5]	73 [17.2]	31.434 [0.773]	34.152 [0.068]	2.681 [0.779]	29 [7.0]
P2	16 [4.1]	100 [11.4]	91 [14.6]	31.184 [0.049]	34.116 [0.049]	2.895 [1.103]	28 [3.9]
P3	11 [4.8]	96 [14.3]	88 [10.1]	29.12 [0.539]	34.045 [0.12]	5.09 [0.415]	45 [3.4]
Amundsen basin							
P1	25 [7.6]	93 [11.1]	68 [15.1]	32.646 [0.630]	34.231 [0.069]	1.583 [0.691]	17 [6.2]
P2	22 [4.0]	95 [8.9]	68 [12.7]	32.087 [1.087]	34.097 [0.042]	1.970 [0.961]	23 [3.7]
P3	16 [4.7]	94 [12.3]	77 [10.3]	32.050 [0.479]	34.023 [0.114]	2.006 [0.374]	20 [3.1]

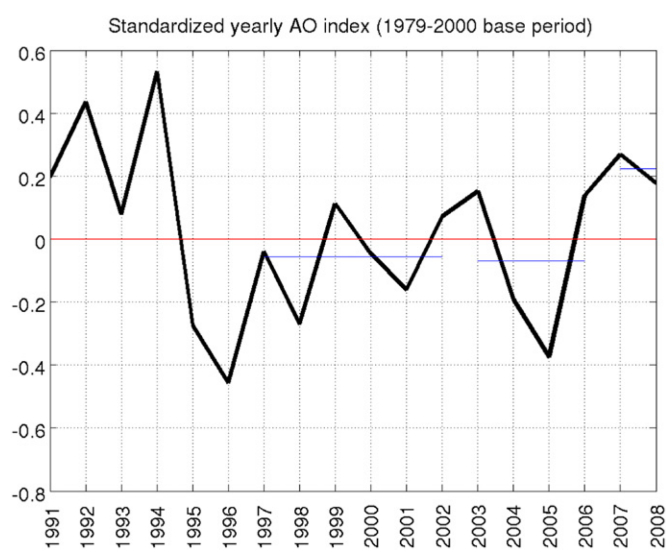

Fig. 11. Standardized yearly AO index (1979–2000 base period) time series, from 1991 to 2008 (downloaded from the NCEP website). The averaged AO index values for period 1, period 2 and period 3 are indicated by blue lines. (For interpretation of the references to color in this figure legend, the reader is referred to the web version of this article.)

the Siberian river runoff spread over the deep Arctic basin. In point of fact, the anomalous eastward component of the winds along the Laptev Sea due to the high AO index of the early 1990s was responsible for the apparent "CHL retreat" reported by Steele and Boyd (1998). Another period of high positive AO index happened during the IPY (Fig. 11). This is coherent with a strong freshening of the mixed layer salinity in the East Siberian Seas and the Makarov basin, and a defreshening at the junction between the Laptev Sea and the Lomonosov ridge (see Fig. 10). However, the Makarov basin is not the only region where the surface salinity dropped during IPY. The Beaufort Gyre, well known as the largest feature accumulating freshwater in the Arctic, was also strongly affected by a freshening. McPhee et al. (2009) found that the freshwater content (relative to 34.8 psu), evaluated in 2008 in the Canada and Makarov basins, increased by 8500 km^3 compared to the climatology.

5.2. The Atlantic water and the halocline base variability

During period 2, the halocline base moved upwards significantly in the Beaufort Gyre, south of 83°N (see Fig. 9 and Table 2). This was a consequence of enhanced heat content at depth due to the arrival of a warm Atlantic water signal in this region. In fact, the Warm Atlantic Water (WAW) of the early 1990s first detected in the Nansen basin (Quadfasel et al., 1991), was observed again north and west of the Chuckchi Plateau in 1998 (McLaughlin et al., 2004). McLaughlin et al. (2004) interpreted thermohaline intrusions as resulting from a mixing of WAW with cool ambient Canadian water, and she also noticed that the WAW had not penetrated the Beaufort Gyre yet. When analyzing the data set located in that region, we detected thermohaline intrusions in the TS curves during P2 (August 2005, see Fig. 12), while none of them were present in the TS curves

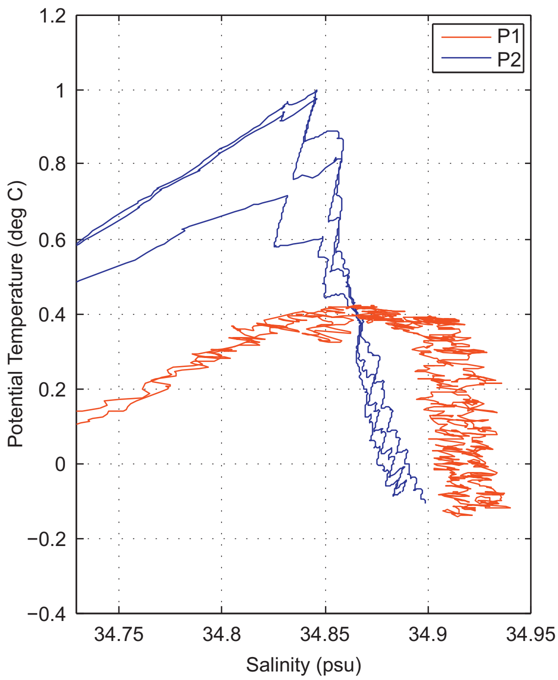

Fig. 12. TS diagram of the profiles located in the Beaufort Gyre during P1 (in red) and P2 (in blue). (For interpretation of the references to color in this figure legend, the reader is referred to the web version of this article.)

during P1 (September 1997). Moreover, the thermohaline intrusions in the TS curves during P2 were similar to the intrusions encountered close to the Chuckchi Plateau and analyzed by McLaughlin et al. (2004). Therefore, a warming at depth, created by the arrival of the WAW in the Beaufort Gyre during P2, forced the halocline base to become shallower.

5.3. Brine release influencing the halocline

The Arctic Ocean Halocline is also influenced by brine rejection. Fig. 13 shows a profile recorded by one of the Polar Ocean Profiling System (POPS) profiler close to the Laptev Sea (83.51°N, 136.7°E) at the end of October 2006. One can see that between 50 and 100 dbar, the temperature reached a minimum while the salinity increased locally before merging in the salinity profile below 100 dbar. These changes were clearly the signature of the presence of brine that locally increased the salt content of the water column and decreased its temperature. This can also be seen in the TS space where the TS diagram is at its freezing point at salinity close to 33.8 psu. This suggests that local processes also play an important role in the halocline variability in addition to large scale advections.

5.4. The seasonal signal impact on the halocline

The previous analysis was based on summer data only in order to eliminate any seasonal bias in the interannual spatiotemporal variability of the halocline properties over the three time periods.

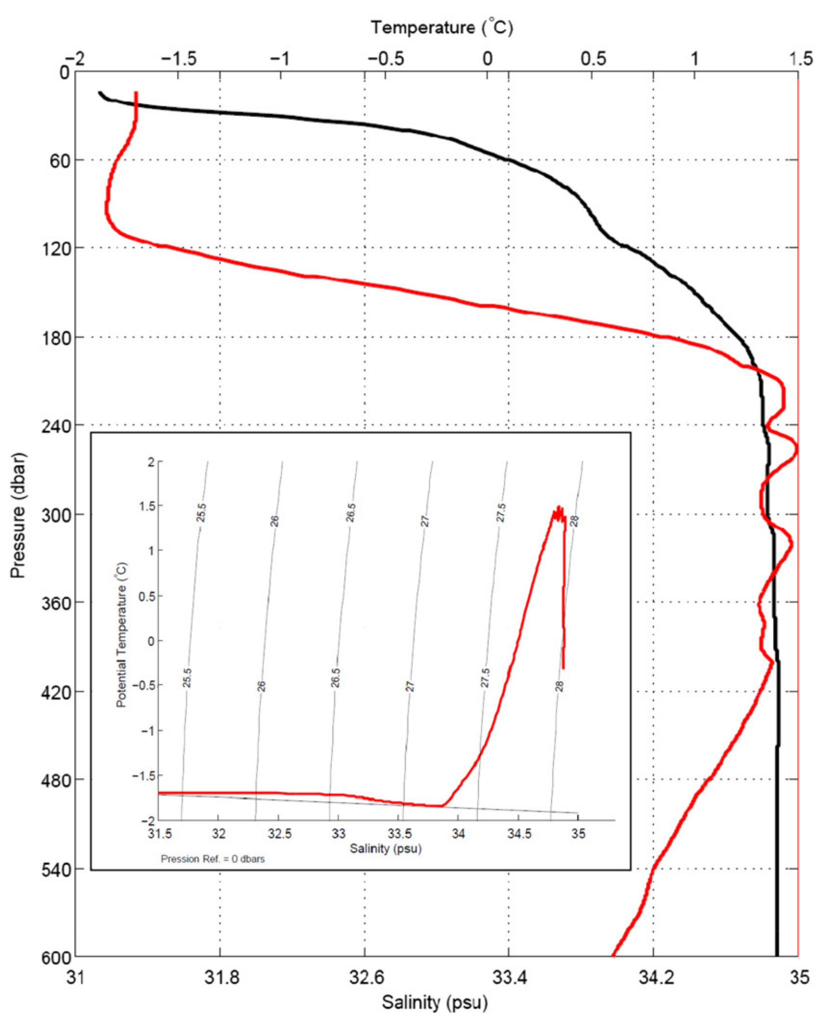

Fig. 13. Temperature (in red) and Salinity (in black) profile and TS diagram of the profile of the 2006/10/29 located close to the Laptev Sea. (For interpretation of the references to color in this figure legend, the reader is referred to the web version of this article.)

However, one might ask does the conclusions deduced from summertime observations still hold during wintertime? Despite the fact that such analysis based on winter data only is not possible because of the poor sampling of winter data before IPY, an indication is given when comparing the analysis of the data set including both winter and summer data. The comparisons between the two analysis revealed no significant impact on the conclusions of the paper indicating that the analysis might not be dependent on the season.

6. Conclusions

We propose a new parametric definition for the Arctic halocline in a Pan Arctic sense, taking into account all the basic elements characterizing the halocline layer. It is based on the fact that the halocline is a thick layer characterized by a salinity gradient all the way from the top to the base of the halocline layer. The halocline stratification is characterized by a mean Brunt Vaisala frequency squared over the halocline thickness. Such a choice allows us to consider both the role of the salinity amplitude and the thickness on the halocline stratification changes. The halocline variability was investigated based on data collected over the entire deep Arctic basin and split into three time periods running from 1997 to 2008.

Observations reveal that the halocline in the Amundsen basin underwent very small variations in stratification, so we can consider it as a rather stable feature over the three time periods in this region. In contrast, the Canada and Makarov basins' halocline became much more stratified during the IPY mainly because of an intense surface water freshening. Observations also confirmed that the impact of the halocline thickness variability on the stratification variability has an important role. It balances the effect of the salinity amplitude in the Canada basin from P1 to P2 and even overcomes it in the Amundsen basin from P2 to P3.

Observations suggest that recent variations in surface salinity observed in the Makarov basin, characterized by a strong freshening during IPY, might be linked to the atmospheric forcing, the AO or any changes in the atmospheric circulation (Dipole Anomaly, Wu et al., 2006). According to Steele and Boyd (1998), the atmospheric forcing is more likely to be responsible for the change in destination of the fresh Siberian shelf waters flowing into the deep Arctic Ocean. More locally, some observations point out that brine rejection could be the process responsible for the salt content variability at depth and, as a consequence, for the variability of the halocline, in addition to the diffusion of heat and salt carried out by the Atlantic water mass underneath. Consequently, both large scale and small scale processes might influence the halocline.

At a time of drastic changes observed in Arctic sea ice cover, and in contrast with the highly variable and strongly perturbed atmosphere, the Arctic Ocean halocline still remained stable and robust. No "retreat" or "disappearance" of the halocline was observed in the Arctic Ocean in spite of a spatiotemporal variability due to both the atmospheric forcing and small scale processes. This suggests that the Atlantic water heat content remained trapped at depth and therefore did not contribute significantly to the drastic changes observed at the surface, at least for the time being.

As a consequence, most of the oceanic implication in the recently observed Arctic sea ice variability might then be linked to the heating of the upper ocean layers by incoming solar radiation (Toole et al., 2010), and to a lesser extent, to the advection of warm Summer Pacific waters at shallow depth (Shimada et al., 2006; Woodgate et al., 2009).

Acknowledgments

Many thanks to people who accepted to share with us their CTD data. Among them are T. Kikuchi (for the Jamstec data), G. Bjork and J.H. Swift (Beringia cruise), I. Ashik (Akademik Fedorov cruises and NP35), D. Kadko and D. Chayes (SCICEX cruises), etc. The Ice-Tethered Profiler data were collected and made available by the Ice-Tethered Profiler Program based at the Woods Hole Oceanographic Institution (http://www.whoi.edu/itp). The NPEO Aerial Survey data and some of the SCICEX cruises data were provided by NCAR/EOL under sponsorship of the National Science Foundation (http://data.eol.ucar.edu/). Many data come from the DAMOCLES project financed by the European Union in the 6th Framework Programme for Research and Development. Finally, we are very grateful to the Geovariances compagy for advises and help about the Kriging interpolation theory and process on ISATIS software. The PhD is supported by the AXA Research Fund. The printed version of this paper is supported by the ACCESS project, an European Project supported within the Ocean of Tomorrow call of the European Commission Seventh Framework Programme.

References

Aagard, K., Coachman, L.K., Carmack, E., 1981. On the halocline of the Arctic Ocean. Deep Sea Res., Part A 28, 529–545.

Bjork, G., Soderkvist, J., Winsor, P., Nikolopoulos, A., Steele, M., 2002. Return of the cold halocline layer to the Amundsen basin of the Arctic Ocean: Implications for the sea ice mass balance. GRL 29 (11), 1513. doi:10.1029/2001GL014157.

Boyd, T.J., Steele, M., Muench, R.D., Gunn, J.T., 2002. Partial recovery of the Arctic Ocean halocline. GRL 29 (14), 1657. doi:10.1029/2001GL014047.

Francis, J.A., Hunter, E., Key, J.R., Wang, X., 2005. Clues to variability in Arctic minimum sea ice extent. GRL 32, L21501. doi:10.1029/2005GL024376.

Jones, E.P., Anderson, L.G., 1986. On the origin of the chemical properties of the Arctic Ocean halocline. J. Geophys. Res. 91 (10), 759–767.

Kikuchi, T., Hatakeyama, K., Morison, J.H., 2004. Distribution of convective lower halocline water in the eastern Arctic Ocean. J. Geophys. Res. 109, C120301. doi:10.1029/2003JC002223.

Krige, D.G., 1951. Une Approche Statistique à Quelques Evaluations de Mine et Problèmes Alliés Chez le Witwatersrand. Thèse Principale de l'université de Witwatersrand.

Kwok, R., Rothrock, D.A., 2009. Decline in Arctic sea ice thickness from submarine and ICE sat records: 1958–2008. GRL 36, L15501. doi:10.1029/2009GL039035.

Matheron, G., 1963. Principes de geostatistics. Géol. Econ. 58, 1246–1266.

McLaughlin, F.A., Carmack, E.C., Macdonald, R.W., Melling, H., Swift, J.H., Wheeler, P.A., Sherr, B.F., Sherr, E.B., 2004. The joint roles of Pacific and Atlantic origin waters in the Canada basin, 1997–1998. Deep Sea Res. I 51, 107–128.

McPhee, M.G., Proshutinsky, A., Morison, J.H., Steele, M., Alkire, B., 2009. Rapid change in freshwater content of the Arctic Ocean. GRL 36, L10602. doi:10.1029/GL037525.

Morison, J., Dungan Smith, J., 1981. Seasonal variations in the upper Arctic Ocean as observed at T-3. GRL 8 (7), 753–756.

Polyakov, I.V., Timokhov, L.A., Alexeev, V.A., Bacon, S., Dmitrenko, I.A., Fortier, L., Folov, I.E., Gascard, J.C., Hansen, E., Ivanov, V.V., Laxon, S., Mauritzen, C., Perovich, D., Shimada, K., Simmons, H.L., Sokolov, V.T., Steele, M., Toole, J., 2010. Arctic Ocean warming contributes to reduced polar ice cap. JPO, 10.1175/2010JPO4339.

Quadfasel, D.A., Sy, A., Wells, D., Tunik, A., 1991. Warming in the Arctic. Nature 350, 385.

Rudels, B., Anderson, L.G., Jones, E.P., 1996. Formation and evolution of the surface mixed layer and halocline of the Arctic Ocean. J. Geophys. Res. 101, 8807–8821.

Rudels, B., Jones, E.P., Schauer, U., Eriksson, P., 2004. Atlantic sources of the Arctic Ocean surface and halocline waters. Polar Res. 23, 181–208.

Rudels, B., 2010. Constraints on exchanges in the Arctic Mediterranean—do they exist and can they be of use? Sandström–Walin Special Secion. Tellus 62A, 109–122.

Shimada, K., Itoh, M., Nishino, S., McLaughlin, F., Carmack, E., Proshutinsky, A., 2005. Halocline structure in the Canada basin of the Arctic Ocean. GRL 32, L03605. doi:10.1029/2004GL021358.

Shimada, K., Kamoshida, T., Itoh, M., Nishino, S., Carmack, C., McLaughlin, F., Zimmermann, S., Proshutinsky, A., 2006. Pacific Ocean Inflow: Influence on catastrophic reduction of sea ice cover in the Arctic Ocean. Geophys. Res. Lett. 33, L08605.

Steele, M., Morison, J.H., Curtin, T., 1995. Halocline water formation in the Barents Sea. J. Geophys.Res. 100, 881–894.

Steele, M., Boyd, T., 1998. Retreat of the cold halocline layer in the Arctic Ocean. JGR 103 (C5), 10419–10435.

Steele, M., Morison, J., Ermold, W., Rigor, E., Ortmeyer, M., 2004. Circulation of summer Pacific halocline water in the Arctic Ocean. J. Geophys. Res. 109, C02027. doi:10.1029/2003JC002009.

Toole, J.M., Timmermans, M.-L., Perovich, D.K., Krishfield, R.A., Proshutinsky, A., Richter-Menge, J.A., 2010. Influences of the ocean surface mixed layer and thermohaline stratification on Arctic Sea Ice in the Central Canada basin. J. Geophys. Res. 115, C10018. doi:10.1029/2009JC005660.

Woodgate, R.A., Weingartner, T.J., Lindsay, R., 2009. The 2007 Bering Strait oceanic heat flux and anomalous Arctic sea ice retreat. Geophys. Res. Lett. 37, L01602. doi:10.1029/2009GL041621.

Wu, B., Wang, J., Walsh, J.E., 2006. Dipole Anomaly in the winter Arctic Atmosphere and Its association with sea ice motion. J. Clim. 19, 210–225.